

Functionals of Brownian bridges arising in the current mismatch in D/A-converters

Markus Heydenreich¹ Remco van der Hofstad¹ Georgi Radulov²

October 29, 2018

Abstract

Digital-to-analog converters (DAC) transform signals from the abstract digital domain to the real analog world. In many applications, DAC's play a crucial role.

Due to variability in the production, various errors arise that influence the performance of the DAC. We focus on the current errors, which describe the fluctuations in the currents of the various unit current elements in the DAC. A key performance measure of the DAC is the *Integrated Non-linearity* (INL), which we study in this paper.

There are several DAC architectures. The most widely used architectures are the thermometer, the binary and the segmented architectures. We study the two extreme architectures, namely, the thermometer and the binary architectures. We assume that the current errors are i.i.d. normally distributed, and reformulate the INL as a functional of a Brownian bridge. We then proceed by investigating these functionals. For the thermometer case, the functional is the maximal absolute value of the Brownian bridge, which has been investigated in the literature. For the binary case, we investigate properties of the functional, such as its mean, variance and density.

1 Current mismatch in digital-to-analog converters

Digital-to-Analog converters (DAC) transform signals from the abstract digital domain to the real analog world. For many applications, this conversion enables the usage of the computational power of robust digital electronics. For example, digital audio and video, digital control, and telecommunications are fields that require digital-to-analog conversion. The advantageous intelligence of the applications in these fields is implemented with digital logic, e.g. microprocessors, and used via DA conversion in the real analog world. However, the DAC errors, at the end of the application chain, may decrease the performance of the whole system. Therefore, predicting and controlling these errors is crucial. This requirement is further emphasized in the highly integrated mixed-signal Systems-on-a-Chip (SoC), as we will explain now.

¹Department of Mathematics and Computer Science, Eindhoven University of Technology, 5600 MB Eindhoven, The Netherlands. m.o.heydenreich@tue.nl, r.w.v.d.hofstad@tue.nl

²Department of Electrical Engineering, Eindhoven University of Technology, EH 5.15, 5600 MB Eindhoven, The Netherlands. g.radulov@tue.nl

Nowadays, the SoC system solutions often integrate DAC functionality together with the digital logic for cost effectiveness. This requires optimal usage of the DAC resources while keeping the errors of the DAC within specified margins, primarily because of the two following reasons. Firstly, the price of the mixed-signal SoC includes the price of the DAC resources even when customers are not interested in the DAC functionality. Secondly, if the DAC does not comply with its specifications, then the entire SoC chip should be discarded. By a careful design, the DAC errors mainly arise from the uncertainty in the manufacturing process and, hence, they are random. Therefore, statistical rules are used to predict the overall performance for high-volume chip production. Knowledge is required that accurately links the DAC resources with the DAC error margins. An important example of such a relationship is the dependence of the Digital-to-Analog (D/A) conversion accuracy on the DAC area, i.e. the silicon area of the chip that is used for the DAC. Higher conversion accuracy is achieved for larger chip areas [2, 14]. However, too large areas introduce additional problems which may degrade the conversion accuracy. Thus, precise knowledge and understanding of the relationship between accuracy and chip area is crucial, particularly for high-volume chip systems including DAC. For a general introduction to DAC converters we refer to [2, 9, 18], whereas Razavi [17] also focusses technical aspects.

The D/A conversion is carried out by switching certain analog quantities, such as voltages, currents or charges, ON or OFF. For the sake of simplicity, and without loss of generality, this paper will assume current as a basic analog quantity. The switching process is controlled by the digital input signal $w \in \{0, 1\}^N$, where N is the length of the binary input signal. If all combinations of 0's and 1's between the digital bits produce valid input signals, i.e., $N = \log_2(n + 1)$, then the coding is called *binary* and N is called the *resolution* of the DAC. A DAC that uses binary coding to control its current quantities is called binary DAC. The switched ON current quantities I_{u_i} are summed to construct the analog output signal current I_{out} . We will assume that the current quantities are *random* and that $\{I_{u_j}\}_{j=1}^n$ are i.i.d. random variables. The sum of all current quantities

$$I_{\text{out}_{\max}} = \sum_{j=1}^n I_{u_j} \quad (1.1)$$

is associated to the maximal digital input word $w_n = (1, 1, \dots, 1)$, and is called the full-scale current of the DAC. The smallest meaningful difference in the analog output, defined as the output *least-significant bit* (LSB), is defined as the full-scale current divided by the number of digital input codes, i.e.,

$$I_{\text{lsb}} := \frac{I_{\text{out}_{\max}}}{n}. \quad (1.2)$$

For general DAC, errors can be classified as static or dynamic. We will focus on the *static* errors, which we now introduce.

For every digital input word $w_k \in \{0, 1\}^N$, there is an analog output value I_{out_k} . The code words $w_k \in \{0, 1\}^N$ will be assumed to be ordered. The difference between two adjacent output values would ideally be $\bar{I}_u = \mathbb{E}[I_{u_j}]$, but in practice it deviates due to mismatch errors coming from the uncertainty of the manufacturing process, i.e.

$$I_{\text{out}_k} - I_{\text{out}_{k-1}} = \bar{I}_u + (I_{\text{lsb}} - \bar{I}_u) + \text{DNL}_k \cdot I_{\text{lsb}}, \quad k = 1, \dots, n. \quad (1.3)$$

Here, $I_{\text{lsb}} - \bar{I}_u$ represents the *linear error* which is independent of k , and

$$\text{DNL}_k = \frac{I_{\text{out}_k} - I_{\text{out}_{k-1}} - I_{\text{lsb}}}{I_{\text{lsb}}}. \quad (1.4)$$

is the *differential non-linearity* in I_{lsb} -scale. As the DAC are required to be *linear* devices, the non-linear errors are the main concern. The *integrated non-linearity* (INL) measures the non-linearity of the whole DAC transfer characteristic, i.e., the cumulated individual non-linear errors. This paper concentrates on the INL, as defined for a code w_k by

$$\text{INL}_k := \sum_{i=1}^k \text{DNL}_i = \frac{I_{\text{out}_k} - k \cdot I_{\text{lsb}}}{I_{\text{lsb}}}, \quad k = 1, \dots, n, \quad (1.5)$$

This definition excludes the linear errors by forcing $\text{INL}_0 = \text{INL}_n = 0$ and normalizes INL_k to LSB-scale. The maximal absolute INL over all codes is given by

$$\text{INL}_{\text{max}} := \max_{k=0, \dots, n} |\text{INL}_k|. \quad (1.6)$$

The statistic INL_{max} is an important specification, because it indicates how linear the DAC is. Another important figure is $\text{Yield}_{\text{INL}}$, which indicates how many of the manufactured chips have INL_{max} under certain specified threshold. This is to say, if a DAC manufacturer guarantees certain linearity, then $\text{Yield}_{\text{INL}}$ describes what proportion of the produced chips fall within these specifications.

INL is the most popular DAC specification, see e.g. [9, 18]. Its practical importance is very high in all DAC application fields. This general definition of INL is valid for all DAC architectures, and all DAC resolutions. The most commonly used architectures are the binary, segmented, and thermometer architectures. The segmented architecture interpolates between the binary and the thermometer architectures. In this paper, we consider the two extreme cases of *thermometer* and *binary* DAC architectures. We now describe these DAC architectures.

For a *thermometer* DAC, $I_{\text{out}_k} = I_{\text{out}_k}^{(\text{T})}$ is given by

$$I_{\text{out}_k}^{(\text{T})} = \sum_{j=1}^k I_{u_j}, \quad k = 0, \dots, n. \quad (1.7)$$

For a *binary* DAC, on the other hand, $I_{\text{out}_k} = I_{\text{out}_k}^{(\text{B})}$ is given by

$$I_{\text{out}_k}^{(\text{B})} = \sum_{m=1}^N B_{k,m} \sum_{j=2^{m-1}}^{2^m-1} I_{u_j}, \quad k = 0, \dots, n, \quad (1.8)$$

where the *switching matrix* B is an $n \times N$ -matrix given by

$$B = \begin{pmatrix} 0 & 0 & 0 & 0 & \cdots & 0 \\ 1 & 0 & 0 & 0 & \cdots & 0 \\ 0 & 1 & 0 & 0 & \cdots & 0 \\ 1 & 1 & 0 & 0 & \cdots & 0 \\ 0 & 0 & 1 & 0 & \cdots & 0 \\ \vdots & \vdots & \vdots & \vdots & \ddots & \vdots \\ 1 & 1 & 1 & 1 & \cdots & 1 \end{pmatrix}. \quad (1.9)$$

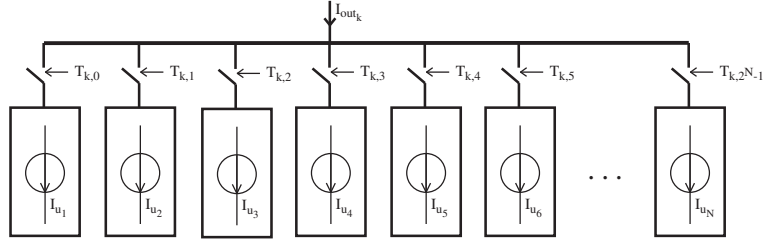


Figure 1: Thermometer DAC. The code word w_k corresponds to switching $T_{k,i}$ ON for $i \leq k$ and switching $T_{k,i}$ OFF for $i > k$.

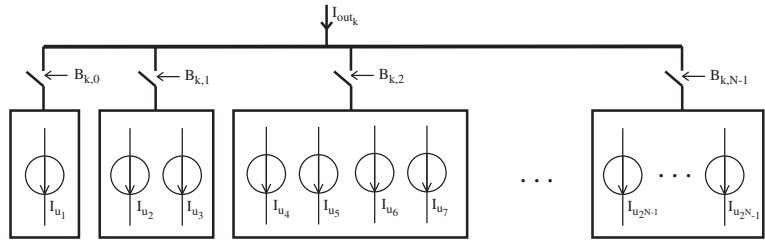


Figure 2: Binary DAC. The code word w_k corresponds to switching those i for which $B_{k,i} = 1$ ON, whereas the i for which $B_{k,i} = 0$ are switched OFF. The matrix B is given in (1.9).

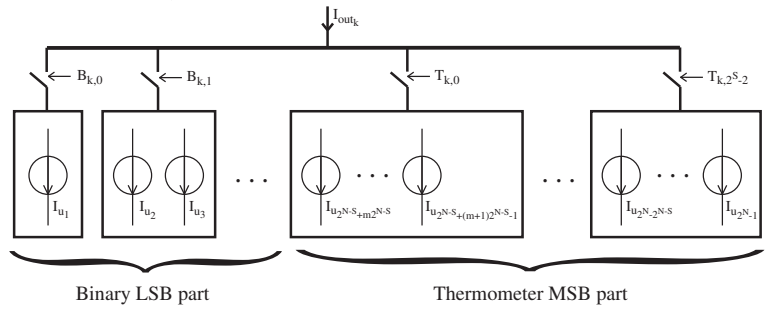


Figure 3: Segmented DAC.

The matrix B is constructed by writing the first n integers in (reversed order) binary coding into the rows of B . Note that the columns of the matrix represent the DAC bits, i.e., the switches of the grouped current sources. The 0's represent switched OFF currents, and the 1's represent switched ON currents. The most left column gives the switches for the least-significant bit current $I_{\text{out}_1}^{(B)} = I_{u_1}$, while the most right column gives the switches for the *most-significant bit* (MSB) current $I_{\text{out}_N}^{(B)} = \sum_{j=2^{N-1}}^{2^N-1} I_{u_j}$. Note that

$$I_{\text{out}_n}^{(B)} = \sum_{m=1}^N B_{n,m} \sum_{j=2^{m-1}}^{2^m-1} I_{u_j} = \sum_{j=1}^n I_{u_j} = nI_{\text{lsb}}, \quad (1.10)$$

so that $\text{INL}_n = 0$.

In practice, the most popular DAC architecture is the segmented one. The segmented DAC architectures implement one part of the input digital bits in a binary way and the other part in a thermometer way. That is how the advantages of both the binary and the thermometer architectures can be combined.

Figure 3 shows a segmented DAC architecture. The LSB part is implemented in a binary way and the MSB part in a thermometer way. The output current for a given level of segmentation S is expressed by

$$I_{\text{out}_k}^{(S)} = \sum_{m=1}^{N-S} B_{k,m} \sum_{j=2^{m-1}}^{2^m-1} I_{u_j} + \sum_{m=1}^{\lfloor k/2^{N-S} \rfloor} \sum_{j=m2^{N-S}}^{(m+1)2^{N-S}-1} I_{u_j}. \quad (1.11)$$

The parameter $S \in \{0, \dots, N\}$ determines the interpolation between the binary and the thermometer parts of the DAC architecture. Indeed, for $S = 0$, the segmented DAC architecture is transformed to a fully binary architecture. On the other hand, for $S = N$, the segmented DAC architecture is transformed to a fully thermometer architecture. Note that in both extreme cases the same unit current sources I_{u_j} are used. Thus, the performance difference is only due to the way the I_{u_j} are combined to construct the output current I_{out_k} . In the binary DAC, the unit currents are first grouped and then switched ON or OFF, while in the thermometer DAC, the unit currents are individually switched ON or OFF. More detailed discussion on DAC architectures can be found in the literature [9, 18, 19].

As discussed, due to manufacturing related mismatch, the currents I_{u_j} always deviate from their designed values, i.e., $I_{u_j} = \bar{I}_u + \varepsilon_j$. The mean value \bar{I}_u is chosen by the DAC designer, whereas ε_j is the random error due to the manufacturing process which we model as an i.i.d. sequence of normal random variable with zero mean and variance σ_u^2 . Nevertheless, our results remain valid when the $\{\varepsilon_j\}$ are i.i.d. distributed with sufficiently many moments. The ratio σ_u/\bar{I}_u is known as the *relative current matching*, i.e., the unit current matching. The relative matching determines the required transistor area for the particular manufacturing process. The smaller σ_u/\bar{I}_u , the more accurate I_{u_j} , but the larger the required area. For more details on the dependence between relative matching and transistor area we refer to [14].

Once σ_u/\bar{I}_u is specified, the required transistor area can be calculated. However, the relationship between σ_u/\bar{I}_u and DAC non-linearity, which is crucial to determine the proportion of chips complying to specifications, has never been determined analytically. So far, DAC engineers have used either Monte Carlo simulations or approximations.

The Monte Carlo simulations of a DAC model produce empirical results to suggest some design specifications σ_u/\bar{I}_u . Although not accurate, this approach is very practical, see [5]. A problem arises for the design of high-resolution DAC, for which N is large. The complexity of the DAC model increases by a factor of two for every additional bit in resolution. For example, for $N = 14$, $n = 16383$ unit elements have to be simulated. Therefore, Monte Carlo simulations are not practical for higher resolutions, because they become complex and slow.

On the other hand, a number of analytical approximations can be found in the literature. The analytical attempts to describe INL, and in particular INL_{\max} , started in 1986. The approach in [11] disregards the correlation between the DAC outputs for different input codes. Bastos [2] proposes a much simpler formula, which considers only the deviation of the transfer characteristic at the mid-scale DAC output, which can be a rough, though simple, estimation of the INL_{\max} . Another approximation was given by van den Bosch et al. [4] by assuming that, if the DAC static transfer characteristic at any code INL has error equal to the target value, e.g., $\text{INL}_k = 0.5 I_{\text{lsb}}$, then there should be a 50% chance that ultimately INL_{\max} is smaller than the target value, i.e., $\text{INL}_k \leq 0.5 I_{\text{lsb}}$ for all k . The major approximation inaccuracy is in the probability that both the positive and negative INL limits are reached for the same DAC sample, e.g., $\text{INL}_k < -0.5 I_{\text{lsb}}$ is disregarded. Though this approach derives a convenient normal distribution for INL_{\max} , it is inaccurate for higher resolutions, as we show in more detail in this paper. In general, approximations lead to transistor over-design, i.e., a transistor area that is too large. In this paper, on the other hand, we shall present an exact analytical formula, for which no approximation is necessary.

Due to the lack of exact analytical formulation of INL and the high complexity of DAC model simulations, the statistics used in industry for a high volume chip production are hard to predict. Here we think of the statistics $\text{Yield}_{\text{INL}}$, the INL_{\max} distribution, INL_{\max} deviation and mean. Furthermore, the advantages of some redundancy based approaches relying on the DAC statistical INL properties cannot be theoretically estimated, see e.g. [16]. Finally, up to now the main DAC architectures, i.e. binary, thermometer, and segmented, cannot be distinguished with respect to their static linearity properties, so they are wrongly considered identical [2, 4]. One conclusion from our results is that the INL for binary and thermometer architectures are *different*.

Implications of the results derived in this paper for the field of DAC's can be found in a second paper [15]. A comparison with the results in [4, 5, 11] is summarized in [15, Table 1].

2 Thermometer coding: Maximum of a Brownian bridge

For the thermometer coding, we can describe the INL as functional of a Brownian bridge as follows.

Theorem 2.1 (INL_{\max} for the *thermometer coding*). *As $n \rightarrow \infty$,*

$$\frac{I_{\text{lsb}}}{\sigma_u \sqrt{n}} \text{INL}_{\max} \longrightarrow X, \quad (2.1)$$

in distribution, in L^1 and L^2 , where the limit X is characterized by

$$X = \max_{t \in [0,1]} |B_t| \quad (2.2)$$

for a Brownian bridge $\{B_s\}_{s \in [0,1]}$, and

$$\mathbb{E}[X] = \frac{\sqrt{2\pi}}{2} \ln 2 \approx 0.86875, \quad \text{Var}(X) = \frac{\pi^2}{12} - \frac{\pi}{2} (\ln 2)^2 \approx 0.0677732, \quad (2.3)$$

and

$$\mathbb{P}(X \leq x) = 1 + 2 \sum_{k=1}^{\infty} (-1)^k e^{-2k^2 x^2}, \quad x > 0. \quad (2.4)$$

Note that in (2.1), we multiply by I_{lsb} rather than by \bar{I}_u . For the convergence in distribution, this makes no difference what so ever, since I_{lsb} converges to \bar{I}_u a.s. by the strong law of large numbers. However, the convergence in L^1 and L^2 fails if we multiply by \bar{I}_u , since in this case, the expected value of $\text{INL}_k = (I_{\text{out}_k} - k \cdot I_{\text{lsb}})/I_{\text{lsb}}$ is not defined, whereas $|\text{INL}_k|$ has infinite mean.

We recall that a Brownian bridge $\{B_s\}_{s \in [0,1]}$ is a Markov process on $[0, 1]$ that is obtained from a Wiener process or Brownian motion in either of the following two ways:

(B1)

$$B_s = W_s - sW_1,$$

where $\{W_s\}_{s \in [0,1]}$ is a Wiener process;

(B2)

$$B_s = W'_s,$$

where $\{W'_s\}_{s \in [0,1]}$ is a Wiener process conditioned on $W'_1 = 0$.

For an introduction to Wiener processes and Brownian bridges we refer to [7]. For the equivalence of (B1) and (B2) cf. [3, pp. 83–85].

Proposition 2.2. *For the thermometer coding,*

$$\max_{k=0, \dots, n} |I_{\text{out}_k}^{(\text{T})} - k I_{\text{lsb}}| \stackrel{\mathcal{D}}{=} \sigma_u \sqrt{n} \max_{k=1, \dots, n} |B_{k/n}|, \quad (2.5)$$

where $\{B_t\}_{t \in [0,1]}$ is a Brownian Bridge process and $\stackrel{\mathcal{D}}{=}$ denotes equality in distribution.

Proof. Since $\{I_{u_j}\}_{j=1, \dots, n}$ is a family of i.i.d. normally distributed random variables with mean \bar{I}_u and variance σ_u^2 , we have that

$$I_{\text{out}_k}^{(\text{T})} - k I_{\text{lsb}} = \sum_{j=1}^k (I_{u_j} - k \bar{I}_u) \quad (2.6)$$

is normally distributed with mean 0 and variance $k\sigma_u^2$. Hence for a Brownian motion $\{W_t\}_{t \geq 0}$,

$$I_{\text{out}_k}^{(\text{T})} - k I_{\text{lsb}} \stackrel{\mathcal{D}}{=} \sigma_u W_k \stackrel{\mathcal{D}}{=} \sigma_u \sqrt{n} W_{k/n}, \quad (2.7)$$

where we used Brownian scaling in the last distributional equality. By substituting $k = n$ and using (1.2) we obtain $n(I_{\text{lsb}} - n\bar{I}_u) \stackrel{\mathcal{D}}{=} \sigma_u \sqrt{n} W_1$. Combined with (2.7), this yields

$$I_{\text{out}_k}^{(\text{T})} - k I_{\text{lsb}} \stackrel{\mathcal{D}}{=} \sigma_u \sqrt{n} \left(W_{k/n} - \frac{k}{n} W_1 \right) \stackrel{\mathcal{D}}{=} \sigma_u \sqrt{n} B_{k/n} \quad (2.8)$$

for a Brownian bridge process $\{B_s\}_{s \in [0,1]}$, where we used (B1) above. After taking absolute values on both sides of (2.8) and the maximum over $k = 1, \dots, n$, we obtain (2.5). \square

The maximum over the discrete time points k/n , $k = 1, \dots, n$, in (2.5) can be replaced by the supremum over the whole interval $[0, 1]$ by using the following lemma:

Lemma 2.3. *For $C > 4$,*

$$\mathbb{P} \left(\left| \max_{k=1, \dots, n} |B_{k/n}| - \max_{t \in [0,1]} |B_t| \right| \geq C \sqrt{\frac{\log n}{n}} \right) \leq 4n^{1-C^2/8} + 2n^{-C^2n/8}. \quad (2.9)$$

In particular, $\max_{k=1, \dots, n} |B_{k/n}|$ converges to $\max_{t \in [0,1]} |B_t|$ in distribution as $n \rightarrow \infty$. Moreover, L^1 - and L^2 -convergence holds.

The proof of Lemma 2.3 is deferred to the appendix. We now use Lemma 2.3 to complete the proof of Theorem 2.1:

Proof of Theorem 2.1. The convergence in (2.1) follows from Lemmas 2.2 and 2.3. For the probability of the upper tail of X (2.4) we refer to [3, (11.39)], the computation of mean and variance of X is straightforward integration. For example, we have that

$$\mathbb{E}[X] = \int_0^\infty \mathbb{P}(X > x) dx = 2 \int_0^\infty \sum_{k=1}^\infty (-1)^{k-1} e^{-2k^2 x^2} dx = 2 \sum_{k=1}^\infty (-1)^{k-1} \frac{\sqrt{2\pi}}{4k} = \frac{\sqrt{2\pi}}{2} \ln 2. \quad (2.10)$$

The interchange of summation and integral can be justified by looking at $X_\varepsilon = X \vee \varepsilon$. \square

3 Binary coding: Block increments of a Brownian bridge

3.1 Results and overview proof

In this section we prove the following theorem characterizing the binary coding statistic.

Theorem 3.1 (INL_{max} for the *binary coding*). *As $n \rightarrow \infty$,*

$$\frac{I_{\text{lsb}}}{\sigma_u \sqrt{n}} \text{INL}_{\text{max}} \longrightarrow M, \quad (3.1)$$

in distribution, in L^1 and L^2 , where the limit M is characterized by

$$M = \frac{1}{2} \sum_{l=1}^\infty 2^{-(l+1)/2} \left| \sum_{j=1}^{l-1} 2^{-(l-j)} Z_j - Z_l \right| \quad (3.2)$$

for a family $\{Z_l\}_{l=1}^\infty$ of i.i.d. standard normal random variables. The expectation of M is given by

$$\mathbb{E}[M] = (2\pi)^{-1/2} \sum_{l=1}^\infty (2^{-l} - 2^{-2l})^{1/2} \approx 0.839792, \quad (3.3)$$

and the variance $\text{Var}(M)$ is computed explicitly in (3.23) below and can be approximated as

$$\text{Var}(M) \approx 0.08007. \quad (3.4)$$

Note that in (3.1), we multiply by I_{lsb} rather than by \bar{I}_u . As explained for Theorem 2.1, this makes no difference for the convergence in distribution, though the convergence in L^1 and L^2 fails.

The proof of Theorem 3.1 is organized as follows. In Lemma 3.3 we prove the convergence in (3.1), where the limit is characterized in terms of increments of Brownian bridges. After this, Proposition 3.4 shows that the weak limit M can be expressed as the weighted sum of standard normal variables, which proves (3.2). Lemma 3.7 states the expression for mean and variance of M . Finally, we give an approximation to the density of M in Section 3.5.

3.2 A Brownian bridge representation of the binary INL_{max}

Our aim is to derive an expression for INL_{max} for the binary coding. First we express the non-linearity of the current steering DAC in terms of a functional of a Brownian bridge.

Lemma 3.2.

$$\max_{k=1, \dots, n} |I_{\text{out}_k}^{(B)} - kI_{\text{lsb}}| \stackrel{\mathcal{D}}{=} \frac{\sigma_u}{2} \sqrt{n} \sum_{m=1}^N \left| B_{\frac{2^m-1}{n}} - B_{\frac{2^{m-1}-1}{n}} \right|, \quad (3.5)$$

where $\{B_s\}_{s=0}^1$ is a Brownian bridge.

Proof. Let $\{W_t\}_{t \in [0, \infty)}$ be a Wiener process, then

$$I_{u_j} - \bar{I}_u \stackrel{\mathcal{D}}{=} \sigma_u \sqrt{n} (W_{j/n} - W_{(j-1)/n}), \quad j = 1, \dots, n, \quad (3.6)$$

where $\stackrel{\mathcal{D}}{=}$ represents equality in distribution. We will further write $=$ rather than $\stackrel{\mathcal{D}}{=}$, because we are interested in the distribution only. Furthermore,

$$I_{\text{lsb}} - \bar{I}_u = \frac{1}{n} \sum_{j=1}^n (I_{u_j} - \bar{I}_u) = \frac{1}{n} \sigma_u W_n = \frac{1}{\sqrt{n}} \sigma_u W_1, \quad (3.7)$$

where we recall that the I_{u_j} are i.i.d. $\mathcal{N}(\bar{I}_u, \sigma_u)$ -distributed.

We want to calculate $I_{\text{out}_k}^{(B)} - kI_{\text{lsb}}$ for k being a power of 2 first. The advantage is that, for $k = 2^{m-1}$, only the m th block $\{I_{u_j} | j = 2^{m-1}, \dots, 2^m - 1\}$ contributes:

$$\begin{aligned} I_{\text{out}_{2^{m-1}}}^{(B)} - 2^{m-1} I_{\text{lsb}} &= \left(I_{\text{out}_{2^{m-1}}}^{(B)} - 2^{m-1} \bar{I}_u \right) + 2^{m-1} (\bar{I}_u - I_{\text{lsb}}) \\ &= \sum_{j=2^{m-1}}^{2^m-1} (I_{u_j} - \bar{I}_u) + 2^{m-1} (\bar{I}_u - I_{\text{lsb}}) \\ &= \sigma_u \sqrt{n} \left(\left(W_{\frac{2^m-1}{n}} - \frac{2^m-1}{n} W_1 \right) - \left(W_{\frac{2^{m-1}-1}{n}} - \frac{2^{m-1}-1}{n} W_1 \right) \right) \\ &= \sigma_u \sqrt{n} \left(B_{\frac{2^m-1}{n}} - B_{\frac{2^{m-1}-1}{n}} \right), \end{aligned}$$

where, in the last line, we used the representation (B1) of Brownian bridges.

For calculating $\max_{k=1,\dots,n} |I_{\text{out}_k}^{(B)} - k I_{\text{lsb}}|$, we need to take the maximum over every configuration of contributing blocks, hence

$$\max_{k=1,\dots,n} |I_{\text{out}_k}^{(B)} - k I_{\text{lsb}}| = \sigma_u \sqrt{n} \underbrace{\max_{\mathfrak{J} \subset \{1,\dots,N\}} \left| \sum_{m \in \mathfrak{J}} B_{\frac{2^m-1}{n}} - B_{\frac{2^{m-1}-1}{n}} \right|}_{:=M_N}. \quad (3.8)$$

We denote by \mathfrak{J}^* the subset of $\{1, \dots, N\}$ for which the maximum in (3.8) is achieved, and use the abbreviation

$$\hat{B}_{n,m} := B_{\frac{2^m-1}{n}} - B_{\frac{2^{m-1}-1}{n}}, \quad m = 1, \dots, N, \quad (3.9)$$

for the increment of the Brownian bridge on the interval $[\frac{2^{m-1}-1}{n}, \frac{2^m-1}{n}]$. Without loss of generality, we may assume that $\sum_{m \in \mathfrak{J}^*} \hat{B}_{n,m}$ is positive, otherwise the same argument for $-B$ holds. Clearly,

$$m \in \mathfrak{J}^* \quad \Leftrightarrow \quad \hat{B}_{n,m} \geq 0. \quad (3.10)$$

Furthermore,

$$0 = B_1 - B_0 = \sum_{m=1}^N \hat{B}_{n,m} = \sum_{m=1}^N \hat{B}_{n,m} \mathbb{1}_{\hat{B}_{n,m} \geq 0} + \sum_{m=1}^N \hat{B}_{n,m} \mathbb{1}_{\hat{B}_{n,m} \leq 0}. \quad (3.11)$$

Using (3.10) in the first line and (3.11) in the second, we obtain

$$\begin{aligned} M_N &= \sum_{m=1}^N \hat{B}_{n,m} \mathbb{1}_{\hat{B}_{n,m} \geq 0} \\ &= \frac{1}{2} \sum_{m=1}^N \hat{B}_{n,m} \mathbb{1}_{\hat{B}_{n,m} \geq 0} + \frac{1}{2} \sum_{m=1}^N (-\hat{B}_{n,m}) \mathbb{1}_{\hat{B}_{n,m} \leq 0} \\ &= \frac{1}{2} \sum_{m=1}^N |\hat{B}_{n,m}|, \end{aligned}$$

which is (3.5). □

We write

$$M_N = \frac{1}{\sigma_u \sqrt{n}} \max_{k=1,\dots,n} |I_{\text{out}_k}^{(B)} - k I_{\text{lsb}}| \quad (3.12)$$

as in (3.8), and define

$$\tilde{M} := \frac{1}{2} \sum_{l=1}^{\infty} |B_{2^{-(l-1)}} - B_{2^{-l}}|, \quad (3.13)$$

where B denotes a Brownian bridge.

Lemma 3.3. *There exists a constant $C > 0$, such that*

$$\mathbb{P} \left(|M_N - \tilde{M}| > \varepsilon \right) \leq \frac{CN^2}{\varepsilon} 2^{-N/2} \quad (3.14)$$

for every $\varepsilon > 0$. In particular, M_N converges to \tilde{M} in distribution as $N \rightarrow \infty$. Moreover, it converges in L^1 and in L^2 .

We show in Proposition 3.4 below that $\tilde{M} \stackrel{\mathcal{D}}{=} M$. The proof of Lemma 3.3 is deferred to the appendix. The combination of Lemmas 3.2 and 3.3 yields the convergence

$$\frac{1}{\sigma_u \sqrt{n}} \max_{k=1, \dots, n} \left| I_{\text{out}_k}^{(B)} - k I_{\text{lsb}} \right| \longrightarrow \frac{1}{2} \sum_{l=0}^{\infty} |B_{2^{-l}} - B_{2^{-(l+1)}}| \quad (3.15)$$

in distribution, in L^1 and L^2 , as $N \rightarrow \infty$ (and thus also $n = 2^N - 1 \rightarrow \infty$). This proves (3.1).

3.3 A representation of M in terms of i.i.d. standard normals

In this section, we will prove the following representation formula, which expresses M in terms of independent standard normal random variables.

Proposition 3.4 (Rewrite of \tilde{M} in terms of standard normals). *Let Z_1, Z_2, \dots be a sequence of i.i.d. standard normal distributed random variables. Then, \tilde{M} can be expressed as*

$$\tilde{M} \stackrel{\mathcal{D}}{=} \frac{1}{2} \sum_{l=1}^{\infty} 2^{-(l+1)/2} \left| \sum_{j=1}^{l-1} 2^{-(l-j)} Z_j - Z_l \right|. \quad (3.16)$$

In other words, \tilde{M} in (3.13) has the same distribution as M in (3.2).

In order to obtain the limit law of \tilde{M} , we have made use of the representation (B1) of the Brownian bridge. Now we will primarily use (B2). We will essentially use the following well-known property of Brownian motion:

Lemma 3.5 (The conditional law of the middle point). *Let $\{W_s\}_{s=0}^{\infty}$ be a standard Brownian motion. Then, the distribution of $W_{\frac{t}{2}}$ conditional on $W_t = z$ is a normal distribution with mean $\frac{z}{2}$ and variance $\frac{t}{4}$.*

Lemma 3.6 (The distribution of $\{B_{2^{-l}}\}_{l=1}^{\infty}$). *The distribution of $\{B_{2^{-l}}\}_{l=1}^{\infty}$ is equal to*

$$B_{2^{-l}} = \sum_{j=1}^l 2^{-(j+1)/2 - (l-j)} Z_j, \quad (3.17)$$

where $\{Z_j\}_{j=1}^{\infty}$ are independent and identically distributed standard normal random variables.

Proof. The proof is by induction in l . For $l = 1$, we use Lemma 3.5 together with the fact that $\{B_s\}_{s=0}^1$ is a Brownian motion conditioned on $B_1 = 0$. This implies that the distribution of $B_{\frac{1}{2}}$ is equal to a normal random variable with mean 0 and variance $\frac{1}{4}$. Therefore,

$$B_{\frac{1}{2}} = \frac{1}{2} Z_1, \quad (3.18)$$

where Z_1 is a standard normal distribution. This initializes the induction hypothesis. To advance it, assume that

$$B_{2^{-(l-1)}} = \sum_{j=1}^{l-1} 2^{-(j+1)/2 - (l-1-j)} Z_j. \quad (3.19)$$

Then, again using Lemma 3.5, the distribution of $B_{2^{-l}}$ conditionally on $B_{2^{-(l-1)}}$ is a normal distribution with mean $1/2 B_{2^{-(l-1)}}$ and variance $2^{-(l+1)}$. Therefore, if we denote $Z_l = 2^{(l+1)/2}(B_{2^{-l}} - \frac{1}{2}B_{2^{-(l-1)}})$, then Z_l is a standard normal random variable independent of $B_{2^{-(l-1)}}$. As a consequence, we have that

$$B_{2^{-l}} = 2^{-(l+1)/2}Z_l + \frac{1}{2}B_{2^{-(l-1)}} = \sum_{j=1}^l 2^{-(j+1)/2-(l-j)}Z_j, \quad (3.20)$$

where in the last step, we have used the induction hypothesis. \square

Proof of Proposition 3.4. As a consequence of Lemma 3.6, we obtain the identity

$$B_{2^{-(l-1)}} - B_{2^{-l}} = \sum_{j=1}^{l-1} 2^{-(j+1)/2-(l-j)}Z_j - 2^{-(l+1)/2}Z_l \quad (3.21)$$

Thus, by (3.13), we obtain (3.16). \square

3.4 The moments of M

In this section, we identify the first two moments of M :

Lemma 3.7 (Moments of M). *The expectation of M is given by (3.3), that is*

$$\mathbb{E}[M] = \frac{1}{\sqrt{2\pi}} \sum_{l=1}^{\infty} (2^{-l} - 2^{-2l})^{1/2} \approx 0.839792, \quad (3.22)$$

and the variance by

$$\text{Var}(M) = \frac{1}{\pi} \sum_{1 \leq l < k} (2^{-l} - 2^{-2l})^{1/2} (2^{-k} - 2^{-2k})^{1/2} \left(\sqrt{1 - \rho_{lk}^2} - 1 + \rho_{lk} \arcsin(\rho_{lk}) \right) + \frac{1}{6} \left(1 - \frac{2}{\pi} \right) \quad (3.23)$$

with

$$\rho_{lk} = \frac{-2^{-(l+k)}}{\sqrt{2^{-l} - 2^{-2l}} \sqrt{2^{-k} - 2^{-2k}}}. \quad (3.24)$$

The variance of M can be approximated by $\text{Var}(M) \approx 0.080066$.

In the proof of Lemma 3.7, we will make use of the following property of the bivariate normal distribution:

Lemma 3.8 (The expected product of absolute values of normals). *Let Y_1, Y_2 be two standard normal random variables having a bivariate normal joint distribution with correlation coefficient ρ . Then*

$$\mathbb{E}[|Y_1||Y_2|] = \frac{2}{\pi} \sqrt{1 - \rho^2} + \frac{2\rho}{\pi} \arctan \left(\frac{\rho}{\sqrt{1 - \rho^2}} \right) = \frac{2}{\pi} \left(\sqrt{1 - \rho^2} + \rho \arcsin(\rho) \right). \quad (3.25)$$

For a proof of Lemma 3.8 see e.g. [10, Exercice 15.6].

Proof of Lemma 3.7. The expression for the mean is easily derived. We note that

$$N_l := B_{2^{-(l-1)}} - B_{2^{-l}} = \sum_{j=1}^{l-1} 2^{-(j+1)/2-(l-j)} Z_j - 2^{-(l+1)/2} Z_l \quad l = 1, 2, \dots \quad (3.26)$$

is normally distributed with mean 0 and variance

$$v_l = \sum_{j=1}^l 2^{-(j+1)-2(l-j)} = 2^{-l} - 2^{-2l}, \quad (3.27)$$

and rewrite M in (3.2) as $M = \frac{1}{2} \sum_{l=1}^{\infty} |N_l|$. Since, for a normal random variable Z with mean 0 and variance σ^2 , we have that

$$\mathbb{E}[|Z|] = \sqrt{\frac{2\sigma^2}{\pi}}, \quad (3.28)$$

the representation formula (3.16) allows us to identify the mean of the random variable M as

$$\mathbb{E}[M] = \frac{1}{2} \sum_{l=1}^{\infty} \mathbb{E}[|N_l|] = \frac{1}{\sqrt{2\pi}} \sum_{l=1}^{\infty} \sqrt{v_l} = \frac{1}{\sqrt{2\pi}} \sum_{l=1}^{\infty} (2^{-l} - 2^{-2l})^{1/2} \approx 0.839792. \quad (3.29)$$

For the variance of M we expand

$$\text{Var}(M) = \frac{1}{4} \left(2 \sum_{1 \leq l < k} \text{Cov}(|N_l|, |N_k|) + \sum_{l=1}^{\infty} \text{Var}(|N_l|) \right). \quad (3.30)$$

The variance term is not too hard, as

$$\text{Var}(|N_l|) = (\mathbb{E}[N_l^2] - \mathbb{E}[|N_l|]^2) = \left(1 - \frac{2}{\pi}\right) v_l, \quad (3.31)$$

and therefore,

$$\sum_{l=1}^{\infty} \text{Var}(|N_l|) = \left(1 - \frac{2}{\pi}\right) \sum_{l=1}^{\infty} (2^{-l} - 2^{-2l}) = \frac{2}{3} \left(1 - \frac{2}{\pi}\right). \quad (3.32)$$

Fix now $1 \leq l < k$. Then

$$\begin{aligned} \text{Cov}(N_l, N_k) &= \text{Cov} \left(\sum_{j=1}^{l-1} 2^{-(j+1)/2-(l-j)} Z_j - 2^{-(l+1)/2} Z_l, \sum_{j=1}^l 2^{-(j+1)/2-(l-j)} Z_j \right) \\ &= \sum_{j=1}^{l-1} 2^{-(j+1)-(l-j)-(k-j)} - 2^{-(l+1)-(k-l)} = -2^{-(l+k)}. \end{aligned} \quad (3.33)$$

Therefore, (N_l, N_k) is a bivariate normal distribution with mean $(0, 0)$, variances (v_l, v_k) , and correlation coefficient

$$\rho_{lk} = \frac{\text{Cov}(N_l, N_k)}{\sqrt{\text{Var}(N_l)} \sqrt{\text{Var}(N_k)}} = \frac{-2^{-(l+k)}}{\sqrt{2^{-l} - 2^{-2l}} \sqrt{2^{-k} - 2^{-2k}}}. \quad (3.34)$$

Denoting (Y_l, Y_k) a bivariate normal distribution with means 0, variances 1 and correlation coefficient ρ_{lk} , we have

$$\begin{aligned} \text{Cov}(|N_l|, |N_k|) &= \sqrt{v_l v_k} \text{Cov}(|Y_l|, |Y_k|) \\ &= \sqrt{v_l v_k} (\mathbb{E}[|Y_l||Y_k|] - \mathbb{E}[|Y_l|] \mathbb{E}[|Y_k|]) \\ &= \sqrt{v_l v_k} \left(\mathbb{E}[|Y_l||Y_k|] - \frac{2}{\pi} \right). \end{aligned} \quad (3.35)$$

By Lemma 3.8, as well as (3.30)–(3.35), we obtain

$$\text{Var}(M) = \frac{1}{\pi} \sum_{1 \leq l < k} \sqrt{v_l v_k} \left(\sqrt{1 - \rho_{lk}^2} - 1 + \rho_{lk} \arcsin(\rho_{lk}) \right) + \frac{1}{6} \left(1 - \frac{2}{\pi} \right). \quad (3.36)$$

Using (3.27) and (3.34) we can approximate $\text{Var}(M)$ numerically, which yields (3.4). \square

Having completed the proofs of (3.1)–(3.4), the proof of Theorem 2.1 is complete.

3.5 Approximating the density of M

We now derive a formula for the density of M . Without loss of generality, we may assume that $\bar{I}_u = 0$ and $\sigma_u = 1$, i.e., the I_u are standard normal distributed.

By denoting $\mathbf{N} = (N_1, N_2, \dots)$ and $\mathbf{Z} = (Z_1, Z_2, \dots)$, we rewrite (3.26) with the help of the (infinite) matrix L as $\mathbf{N} = -L \cdot \mathbf{Z}$, where

$$L_{jl} = \begin{cases} -2^{-(j+1)/2-(l-j)} & \text{if } j < l; \\ 2^{-(l+1)/2} & \text{if } j = l; \\ 0 & \text{if } j > l. \end{cases} \quad (3.37)$$

Note that L is a lower triangular matrix.

We will approximate the density of the infinite sum $M = 1/2 \sum_{l=1}^{\infty} |N_l|$ by the finite sum

$$M^{(m)} = \frac{1}{2} \sum_{l=1}^m |N_l|, \quad m \in \mathbb{N}. \quad (3.38)$$

Writing $\mathbf{N}^{(m)} = (N_1, \dots, N_m)$, $\mathbf{Z}^{(m)} = (Z_1, \dots, Z_m)$, and $L^{(m)}$ for the upper left $m \times m$ corner of the infinite matrix L , we have that $\mathbf{N}^{(m)} = -L^{(m)} \cdot \mathbf{Z}^{(m)}$. In particular, $\mathbf{N}^{(m)}$ is normally distributed with mean $(0, \dots, 0)$ and covariance matrix $\Sigma^{(m)} = L^{(m)} \cdot (L^{(m)})^T$, where we write $(L^{(m)})^T$ for the transpose of the matrix $L^{(m)}$. Note that

$$(\Sigma^{(m)})_{jl} = \begin{cases} -2^{-(j+l)} & \text{if } j \neq l \\ 2^{-l} - 2^{-2l} & \text{if } j = l. \end{cases} \quad (3.39)$$

Given the mean and covariance matrix of a multivariate normal distribution, its density is known to be

$$f_{\mathbf{N}^{(m)}}(\mathbf{n}) = \frac{1}{(2\pi)^{m/2}} \frac{1}{(\det \Sigma^{(m)})^{1/2}} \exp \left\{ -\frac{1}{2} \mathbf{n} (\Sigma^{(m)})^{-1} \mathbf{n}^T \right\}, \quad (3.40)$$

where $\mathbf{n} = (n_1, \dots, n_m) \in \mathbb{R}^m$. We write $|\mathbf{N}^{(m)}|$ for the pointwise absolute value $(|N_1|, \dots, |N_m|)$ of the m -dimensional vector $\mathbf{N}^{(m)}$. Its density is given by

$$f_{|\mathbf{N}^{(m)}|}(\mathbf{n}) = \sum_{\sigma \in \{-1, 1\}^m} \frac{1}{(2\pi)^{m/2}} \frac{1}{(\det \Sigma^{(m)})^{1/2}} \exp \left\{ -\frac{1}{2} (\sigma \mathbf{n}) (\Sigma^{(m)})^{-1} (\sigma \mathbf{n})^T \right\}, \quad \mathbf{n} \in [0, \infty)^m, \quad (3.41)$$

where $(\sigma \mathbf{n}) = (\sigma_1 n_1, \dots, \sigma_m n_m)$. See e.g., [1, (6.3.20)].

The determinant $\det \Sigma^{(m)}$ and the inverse $(\Sigma^{(m)})^{-1}$ of the covariance matrix are easy to compute since $L^{(m)}$ is a triangular matrix. The results are stated in the following two lemmas.

Lemma 3.9. *For all $m \in \mathbb{N}$, the determinant of $\Sigma^{(m)}$ is*

$$\det \Sigma^{(m)} = 2^{-m(m+3)/2}. \quad (3.42)$$

Proof. First we note that

$$\det \Sigma^{(m)} = (\det L^{(m)})^2. \quad (3.43)$$

Since $L^{(m)}$ is a triangular matrix, its determinant is obtained by multiplying the entries on the diagonal, and hence

$$\det \Sigma^{(m)} = \left(\prod_{j=1}^m -L_{jj}^{(m)} \right)^2 = \left(\prod_{j=1}^m 2^{-(l+1)/2} \right)^2 = 2^{-m(m+3)/2}. \quad (3.44)$$

□

Lemma 3.10. *For all $m \in \mathbb{N}$, the inverse of $\Sigma^{(m)}$ is given by*

$$(\Sigma^{(m)})_{jl}^{-1} = \begin{cases} (j \wedge l) 2^{(j+l)/2-1} & \text{for } j \neq l; \\ (j+1) 2^{j-1} & \text{for } j = l. \end{cases} \quad (3.45)$$

Proof. Since $L^{(m)}$ is a triangular matrix, it is easy to see that the inverse $(L^{(m)})^{-1}$ is given by

$$(L^{(m)})_{jl}^{-1} = \begin{cases} 2^{(j-1)/2} & \text{if } j > l; \\ 2^{(j+1)/2} & \text{if } j = l; \\ 0 & \text{if } j < l. \end{cases} \quad (3.46)$$

For $j < l$ we have that

$$(\Sigma^{(m)})_{jl}^{-1} = \sum_{k=1}^{j \wedge l} ((L^{(m)})^{-1})_{jk} ((L^{(m)})^{-1})_{lk} = \sum_{k=1}^j 2^{(j-1)/2} 2^{(l-1)/2} = j 2^{(j+l)/2-1}, \quad (3.47)$$

whereas for $j = l$,

$$(\Sigma^{(m)})_{jj}^{-1} = \sum_{k=1}^j ((L^{(m)})^{-1})_{jk}^2 = \sum_{k=1}^{j-1} 2^{(j-1)/2} + 2^{(j+1)/2} = (j+1) 2^{j-1}. \quad (3.48)$$

□

In order to calculate the density of $M^{(m)} = \frac{1}{2}(|N_1| + \dots + |N_m|)$ at $y \geq 0$, we have to integrate (3.40) over the $(m - 1)$ -dimensional surface $\{(n_1, \dots, n_m) \mid 2y = |n_1| + \dots + |n_m|\}$. This leads to the following formula:

$$f_{M^{(m)}}(y) = 2 \int_0^{2y} \int_0^{2y-n_1} \cdots \int_0^{2y-n_1-\dots-n_{m-2}} f_{|N^{(m)}|}(n_1, n_2, \dots, n_{m-1}, (2y - n_1 - \dots - n_{m-1})) \quad (3.49)$$

$$dn_{m-1} \cdots dn_2 dn_1, \quad y \in [0, \infty).$$

Note that there are $m - 1$ integrals. Thus for $m = 1$ there are no integrals and

$$f_{M^{(1)}}(y) = 2f_{|N^{(1)}|}(2y) = 4\sqrt{\frac{2}{\pi}} \exp\{-8y^2\}, \quad y \in [0, \infty). \quad (3.50)$$

Finally, (3.49) gives us a formula for the density of $M^{(m)}$. The only (numerical) problem are the integrals. For larger values of m , an intelligent way of numerical integration seems necessary.

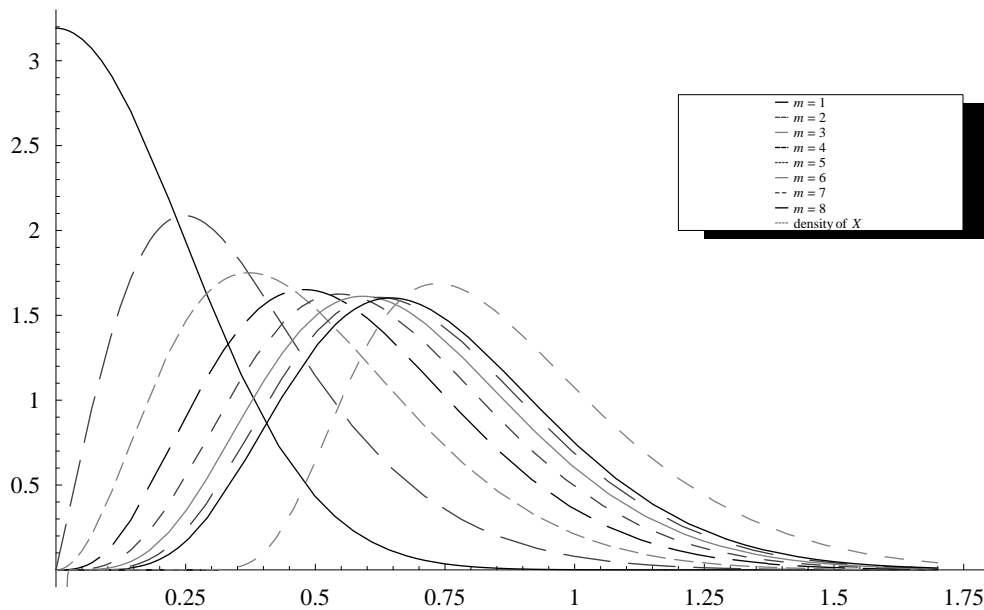


Figure 4: The density of $M^{(m)}$ for different values of m , in contrast to the density of X .

However, for sufficiently small m , a mathematical standard package, such as Mathematica, gives good approximations (see Figure 4).

3.6 A disintegration approach to the density of M

In this subsection we present a different approach to the density of M . We define the quantity

$$\overline{M} = \frac{1}{2} \sum_{l=1}^{\infty} |W_{2-(l-1)} - W_{2-l}| \quad (3.51)$$

for a Wiener process $\{W_s\}_{s \in [0,1]}$. It is obvious that $M \stackrel{D}{=} \overline{M}|_{W_1=0}$, cf. (3.13) and (B2) on page 7. Let \hat{f} be the Fourier transform of the joint distribution of \overline{M} and W_1 , i.e.

$$\hat{f}(k_1, k_2) = \mathbb{E}[\exp\{i(k_1 \overline{M} + k_2 W_1)\}]. \quad (3.52)$$

Using the independence and stationarity of the increments of the Wiener process in (3.51) we obtain

$$\hat{f}(k_1, k_2) = \prod_{l=1}^{\infty} \underbrace{\mathbb{E}[\exp\{i(k_1 |W_{2^{-(l-1)}} - W_{2^{-l}}| + k_2 (W_{2^{-(l-1)}} - W_{2^{-l}}))\}]}_{=\hat{h}_l(k_1, k_2)}, \quad (3.53)$$

where

$$\hat{h}_l(k_1, k_2) = \mathbb{E}[\exp\{i(k_1 |Z| + k_2 Z)\}], \quad (3.54)$$

and Z is a $\mathcal{N}(0, 2^{-l})$ -distributed normal random variable. Once we have computed \hat{h}_l , we obtain the joint density of (\overline{M}, W_1) via inverse Fourier transformation as

$$f_{\overline{M}, W_1}(x, y) = \iint \exp\{-ik_1 x - ik_2 y\} \hat{f}(k_1, k_2) \frac{dk_1 dk_2}{(2\pi^2)^2}. \quad (3.55)$$

The density of M equals the density of \overline{M} conditioned on $W_1 = 0$, whence

$$f_M(x) = \frac{f_{\overline{M}, W_1}(x, 0)}{f_{W_1}(0)} = \sqrt{2\pi} \iint \exp\{-ik_1 x\} \hat{f}(k_1, k_2) \frac{dk_1 dk_2}{(2\pi^2)^2}. \quad (3.56)$$

It remains to calculate $\hat{h}_l(k_1, k_2)$. If we let

$$\hat{h}_l(k) = \mathbb{E}[e^{ikZ} \mathbb{1}_{\{Z \geq 0\}}], \quad (3.57)$$

then $\hat{h}_l(k_1, k_2) = \hat{h}_l(k_1 + k_2) + \hat{h}_l(k_1 - k_2)$. The dependence of \hat{h}_l on l can easily be eliminated by scaling:

$$\hat{h}_l(k) = \hat{h}(2^{-l/2} k), \quad (3.58)$$

where \hat{h} is as in (3.57) with Z being $\mathcal{N}(0, 1)$ -distributed. It can be shown that

$$\hat{h}(k) = \frac{1}{2} e^{-k^2/2} + i \frac{e^{-k^2/2}}{2\sqrt{2\pi}} \int_{-k}^k e^{x^2/2} dx, \quad (3.59)$$

but the inverse Fourier transform in (3.56) seems intractable.

4 Conclusions

We have derived the distribution of the INL_{\max} in terms of Brownian bridges. This distributional identity holds for all architectures, in particular also for the segmented one.

In the thermometer case we have identified the limiting distribution of INL_{\max} as the absolute maximum of Brownian bridges, which is well-known in the literature.

For the binary case, we have identified the limiting distribution of INL_{\max} in terms of a Brownian bridge. We have further provided a representation in terms of independent standard

normal variables and have computed the mean and variance of INL_{\max} . Finally, we have given a procedure that approximates the density.

We want to emphasize that the INL_{\max} in the thermometer case and in the binary case behave differently. Although the densities look alike, e.g. the upper tails are quite close to each other, there are significant changes in the lower tail. The thermometer case has, compared to the binary case, a slightly larger mean, but a slightly smaller variance. Even though the distributions in the two cases are close, they are *not* the same.

We still miss the distribution function for the binary case. Random sums of the type in (3.13) have appeared in the literature. In particular the quantity

$$S = \sum_{l=1}^{\infty} 2^{-l} V_l \quad (4.1)$$

where $\{V_l\}_{l=1}^{\infty}$ are i.i.d. exponential random variables arise in a variety of applications, see e.g. Ott, Kemperman and Mathis [13], Guillemin, Robert and Zwart [8] and Litvak and van Zwet [12]. The density of S can be expressed in terms of an infinite sum, cf. [13, Section 5]. When the summands are independent *uniform* random variables, i.e., $\{V_l\}_{l=1}^{\infty}$ are i.i.d. uniform random variables on $(0, 1)$, the density of S can be computed explicitly [6].

Furthermore, it would be interesting to extend the results to the segmented case. In particular, it would be of interest to investigate which limiting INL_{\max} distribution has the smallest mean. This should correspond to the optimal DAC architecture. Practical implications of our results can be found in a companion paper [15].

A Proof of Lemmas 2.3 and 3.3

Proof of Lemma 2.3. We first prove (2.9). Let $\{B_s\}_{s \in [0,1]}$ be a Brownian bridge. Then,

$$\left| \max_{k=1, \dots, n} |B_{k/n}| - \max_{t \in [0,1]} |B_t| \right| \leq \max_{\substack{k=1, \dots, n \\ t \in [\frac{k-1}{n}, \frac{k}{n}]} |B_{k/n} - B_t| \quad (A.1)$$

Using representation (B1) above, we can further bound (A.1) from above by

$$\max_{\substack{k=1, \dots, n \\ t \in [\frac{k-1}{n}, \frac{k}{n}]} |W_{k/n} - W_t| + \frac{1}{n} |W_1| \quad (A.2)$$

for a Wiener process $\{W_s\}_{s \in [0,1]}$. Using the Markov property and Brownian scaling, we obtain that for $k = 1, \dots, n$,

$$\max_{t \in [\frac{k-1}{n}, \frac{k}{n}]} |W_{k/n} - W_t| \stackrel{\mathcal{D}}{=} \frac{1}{\sqrt{n}} \max_{t \in [0,1]} |W_t|, \quad (A.3)$$

where $\stackrel{D}{=}$ stands for equality in distribution. Hence, for $C > 0$,

$$\begin{aligned} & \mathbb{P}\left(\left|\max_{k=1,\dots,n} |B_{k/n}| - \max_{t \in [0,1]} |B_t|\right| \geq C\sqrt{\frac{\log n}{n}}\right) \\ & \leq \mathbb{P}\left(\max_{k=1,\dots,n} \left\{ \max_{t \in [\frac{k-1}{n}, \frac{k}{n}]} |W_{k/n} - W_t| \geq \frac{C}{2}\sqrt{\frac{\log n}{n}} \right\}\right) + \mathbb{P}\left(\frac{1}{n}|W_1| \geq \frac{C}{2}\sqrt{\frac{\log n}{n}}\right) \\ & \leq n\mathbb{P}\left(\max_{t \in [0,1]} |W_t| \geq \frac{C}{2}\sqrt{\log n}\right) + \mathbb{P}\left(|W_1| \geq \frac{C}{2}\sqrt{n \log n}\right). \end{aligned} \quad (\text{A.4})$$

For the first term, we bound for every $b \geq 0$,

$$\mathbb{P}\left(\max_{t \in [0,1]} |W_t| \geq b\right) \leq 2\mathbb{P}\left(\max_{t \in [0,1]} W_t \geq b\right) = 4\mathbb{P}(W_1 \geq b) \leq 4e^{-b^2/2}, \quad (\text{A.5})$$

where we use the reflection principle [7, Theorem (6), p. 526] in the second and a standard bound on the tail of standard normals in the third step. Substituting $b = C/2\sqrt{\log n}$ we obtain

$$n\mathbb{P}\left(\max_{t \in [0,1]} |W_t| \geq \frac{C}{2}\sqrt{\log n}\right) \leq n4n^{-(C/2)^2/2} = 4n^{1-C^2/8}. \quad (\text{A.6})$$

For the second term in (A.4), we obtain analogously

$$\mathbb{P}\left(|W_1| \geq \frac{C}{2}\sqrt{n \log n}\right) \leq 2\mathbb{P}\left(W_1 \geq \frac{C}{2}\sqrt{n \log n}\right) \leq 2n^{-C^2n/8} \quad (\text{A.7})$$

The bound (A.4), together with (A.6)-(A.7) proves (2.9).

For the convergence in L^1 , we use that, with

$$X_n = \max_{k=1,\dots,n} |B_{k/n}|, \quad X = \max_{t \in [0,1]} |B_t|, \quad (\text{A.8})$$

we have that

$$\mathbb{E}|X_n - X| = \int_0^\infty \mathbb{P}(|X_n - X| \geq t) dt. \quad (\text{A.9})$$

We split between $t \leq 4\sqrt{\frac{\log n}{n}}$ and $t > 4\sqrt{\frac{\log n}{n}}$. For $t \leq 4\sqrt{\frac{\log n}{n}}$, we bound $\mathbb{P}(|X_n - X| \geq t) \leq 1$, while for $t > 4\sqrt{\frac{\log n}{n}}$, we use (A.6) and (A.7) to bound

$$\mathbb{P}(|X_n - X| \geq t) \leq 6ne^{-nt^2/2}. \quad (\text{A.10})$$

Substitution of these bounds yields

$$\mathbb{E}|X_n - X| = \int_0^\infty \mathbb{P}(|X_n - X| \geq t) dt \leq 4\sqrt{\frac{\log n}{n}} + 6n \int_{4\sqrt{\frac{\log n}{n}}}^\infty e^{-nt^2/2} dt = O\left(\sqrt{\frac{\log n}{n}}\right). \quad (\text{A.11})$$

The convergence in L^2 follows similarly, now using

$$\mathbb{E}[(X_n - X)^2] = \int_0^\infty 2t\mathbb{P}(|X_n - X| \geq t) dt. \quad (\text{A.12})$$

We leave the details to the reader. \square

Proof of Lemma 3.3. We observe that, by (3.5), (3.12) and (3.13), and replacing m by $N - m$,

$$\left| M_N - \tilde{M} \right| \leq \sum_{m=1}^{N-1} |B_{2^{-m}} - B_{(2^{N-m}-1)/n}| + \sum_{m=N}^{\infty} |B_{2^{-m}} - B_{2^{-m-1}}|. \quad (\text{A.13})$$

Therefore, for an arbitrary chosen constant $\varepsilon > 0$, we have that

$$\mathbb{P}\left(\left| M_N - \tilde{M} \right| > \varepsilon\right) \leq \underbrace{\mathbb{P}\left(\sum_{m=1}^{N-1} |B_{2^{-m}} - B_{(2^{N-m}-1)/n}| > \frac{\varepsilon}{2}\right)}_{(I)} + \underbrace{\mathbb{P}\left(\sum_{m=N}^{\infty} |B_{2^{-m}} - B_{2^{-m-1}}| > \frac{\varepsilon}{2}\right)}_{(II)}. \quad (\text{A.14})$$

Using representation (B1), we see that for a Brownian bridge $\{B_s\}_{s \in [0,1]}$, and any $0 \leq s < t \leq 1$, the following holds for every constant $C > 0$:

$$\begin{aligned} \mathbb{P}(|B_t - B_s| > C) &\leq \mathbb{P}(|W_t - W_s - (t-s)W_1| > C) \\ &\leq \mathbb{P}(|W_t - W_s| > C/2) + \mathbb{P}(|(t-s)W_1| > C/2). \end{aligned} \quad (\text{A.15})$$

Using the Markov inequality and Gaussian scaling we obtain

$$\mathbb{P}(|B_t - B_s| > C) \leq \frac{2}{C} \sqrt{t-s} \mathbb{E}[|W_1|] + \frac{2}{C}(t-s) \mathbb{E}[|W_1|] \leq \frac{4}{C} \sqrt{\frac{2}{\pi}(t-s)}. \quad (\text{A.16})$$

We use (A.16) to bound (I) in (A.14) from above by

$$\sum_{m=1}^{N-1} \mathbb{P}\left(|B_{2^{-m}} - B_{(2^{N-m}-1)/n}| > \frac{\varepsilon}{2(N-1)}\right) \leq \sum_{m=1}^{N-1} \frac{8(N-1)}{\varepsilon} \sqrt{\frac{1}{2^m} - \frac{2^{N-m}-1}{2^N-1}} \leq \frac{8N^2}{\varepsilon 2^{N/2}}, \quad (\text{A.17})$$

which converges to 0 as $N \rightarrow \infty$. The second term (II) in (A.14) can be bounded using the Markov inequality by

$$(II) \leq \frac{2}{\varepsilon} \mathbb{E}\left[\sum_{m=N}^{\infty} |B_{2^{-m}} - B_{2^{-m-1}}|\right]. \quad (\text{A.18})$$

Using (3.29), this expectation can be computed as

$$\mathbb{E}\left[\frac{1}{2} \sum_{m=N}^{\infty} |B_{2^{-m}} - B_{2^{-m-1}}|\right] = \frac{1}{\sqrt{2\pi}} \sum_{m=N}^{\infty} (2^{-m} - 2^{-2m})^{1/2}, \quad (\text{A.19})$$

and

$$(II) \leq \frac{2\sqrt{2}}{\varepsilon\sqrt{\pi}} \sum_{m=N}^{\infty} (2^{-m} - 2^{-2m})^{1/2} \leq \frac{4}{\varepsilon\sqrt{\pi}(\sqrt{2}-1)} 2^{-N/2} \quad (\text{A.20})$$

which converges to 0 as $N \rightarrow \infty$.

The combination of (A.14), (A.17) and (A.20) shows that, for $C = 8 + 4(\sqrt{2\pi} - \sqrt{\pi})^{-1}$,

$$\mathbb{P}\left(\left| M_N - \tilde{M} \right| > \varepsilon\right) \leq \frac{CN^2}{\varepsilon} 2^{-N/2} \quad (\text{A.21})$$

for every $\varepsilon > 0$, i.e., M_N converges to \tilde{M} in distribution as $N \rightarrow \infty$.

The convergence in L^1 and in L^2 follows as in the proof of Lemma 2.3. \square

Acknowledgement

The work of MH and RvdH was supported by the Netherlands Organisation for Scientific Research (NWO), and the work of GR was supported by STW, project ECS.6098. We thank Marko Boon for help with the simulations in Figure 4. We thank David Brydges for enlightening discussions on multivariate normal distributions, and Olaf Wittich for pointing our attention to the disintegration approach in Section 3.6.

References

- [1] L. J. Bain and M. Engelhardt. *Introduction to Probability and Mathematical Statistics*. Duxbury, second edition, 1991.
- [2] J. Bastos. *Characterization of MOS Transistor Mismatch for Analog Design*. PhD thesis, Katholieke Universiteit Leuven, April 1998.
- [3] P. Billingsley. *Convergence of Probability Measures*. Wiley New York, 1986.
- [4] A. v. d. Bosch, M. Steyaert, and W. Sansen. *Static and Dynamic Performance Limitations for High-Speed D/A Converters*. Kluwer Academic Publications, 2004.
- [5] C. S. G. Conroy, W. A. Lane, M. A. Moran, K. R. Lakshmikumar, M. A. Copeland, and R. A. Hadaway. Comments, with reply, on ‘Characterization and modeling of mismatch in MOS transistors for precision analog design’. *IEEE Journal of Solid-State Circuits*, 23(1):294–296, February 1988.
- [6] A. Fey-den Boer, personal communication.
- [7] G. R. Grimmett and D. R. Stirzaker. *Probability and random processes*. Oxford University Press, New York, third edition, 2001.
- [8] F. Guillemin, P. Robert and B. Zwart. AIMD algorithms and exponential functionals. *Annals of Applied Probability*, 14(1):90–117, 2004.
- [9] P. G. A. Jesper. *Integrated Converters*. Oxford University Press, 2001.
- [10] M. Kendall and A. Stuart. *The Advanced Theory of Statistics*, volume 1. Griffin London, fourth edition, 1977.
- [11] K. Lakshmikumar, R. Hadaway, and M. Copeland. Characterization and modeling of mismatch in MOS transistors for precision analog design. *IEEE Journal of Solid-State Circuits*, 21(6):1057–1066, December 1986.
- [12] N. Litvak and W. R. van Zwet. On the minimal travel time needed to collect n items on a circle. *The Annals of Applied Probability*, 14(2):881–902, 2004.
- [13] T. J. Ott, J. H. B. Kemperman and M. Mathis. The stationary behavior of ideal TCP Congestion Avoidance. Unpublished manuscript, available at <http://www.teunisott.com/Papers>, August 1996.

- [14] M. J. M. Pelgrom, A. C. J. Duinmaijer, and A. P. G. Welbers. Matching properties of MOS transistors. *IEEE Journal of Solid-State Circuits*, 24(5):1433–1439, 1989.
- [15] G. I. Radulov, M. Heydenreich, R. v. d. Hofstad, J. A. Hegt, and A. H. M. v. Roermund. Brownian bridge based statistical analysis of DAC INL caused by current mismatch. *IEEE Transactions on Circuits and Systems II: Express Briefs*, 54 (2): 146–150 (2007).
- [16] G. I. Radulov, P. J. Quinn, P. C. W. van Beek, J. A. Hegt, and A. H. M. van Roermund. A binary-to-thermometer decoder with built-in redundancy for improved DAC yield. In *ISCAS*, Kos, Greece, 2006.
- [17] B. Razavi. *Design of Analog CMOS Integrated Circuits*. McGraw-Hill, 2001.
- [18] R. J. Van de Plassche. *Integrated Analog-to-Digital and Digital-to-Analog Converters*. Kluwer Academic Publishers, 1994.
- [19] J. J. Wikner. *Studies on CMOS Digital-to-Analog Converters*. PhD thesis, Department of Electrical Engineering, Linköping University, 2001.